Autofluorescence and metabolic signatures in a pig model of differentiation based on induced pluripotent cells and embryonic bodies

A.C. Croce,[1] G. Bottiroli,[1] G. Santin,[1] G. Pacchiana,[2] P. Vezzoni,[2] E. Di Pasquale[2]

[1]IGM-CNR and Department of Biology and Biotechnology, University Pavia, Pavia 27100, Italy
[2]Humanitas Clinical and Research Center and IRGB/CNR, UOS of Milan, Rozzano 20089 (MI), Italy

Corresponding author: Anna Cleta Croce
Istituto di Genetica Molecolare del CNR c/o Dipartimento di Biologia e Biotecnologie "L. Spallanzani", via Ferrata, 9
27100, Pavia, Italy
Tel. +39.0382.986428 - Fax +39.0382.986430
E-mail: croce@igm.cnr.it

Summary
Besides several genetic and molecular markers, stem cells undergoing differentiation show changes in their metabolic engagement, such as a switch from anaerobic to aerobic energetic metabolism and decreased autophagic activity, representing metabolic signatures of the stemness status. These activities involve biomolecules - respectively NAD(P)H and flavins, and lipofuscin-like lipopigments- that give rise to autofluorescence (AF) emission under suitable excitation light conditions. Since these endogenous fluorophores can be exploited as cell intrinsic biomarkers, attention is currently deserved to assess the potential of AF analysis to monitor the cell stemness status or maturation degree into a desired phenotype. In our work, we employed pig induced pluripotent stem (iPS) cell as a model of differentiation to compare their AF properties in living conditions with those of embryoid bodies (EBs) derived from them, by means of imaging, microspectrofluorometric techniques and spectral fitting analysis. The AF results indicate that reprogramming of suine iPS cells do not lead to typical metabolic functions of the undifferentiated status. These findings support the value of AF analysis as a tool for a comprehensive assessment of the actual stem cells differentiation degree in the development of regenerative medicine strategies, and for application to animal species of interest in veterinary, zootechnology and, in general, to the species for which immunomarkers are not yet available.

Key words: aerobic/anaerobic metabolism, lipofuscin-like lipopigments, microspectrofluorometry, stem cells.

Introduction

The natural presence of biomolecules acting as endogenous fluorophores is responsible for the autofluorescence (AF) emission rising from cells and tissues when submitted to a suitable excitation light. The strict involvement of endogenous fluorophores in metabolic reactions influences their amount and physicochemical state, in turn affecting their emission properties. As a consequence, the overall cell AF emission signal carries multiple information, making endogenous fluorophores to act as intrinsic biomarkers of the cell functional engagement in the absence of exogenous labeling agents (Ramanujam, 2000; Bottiroli and Croce, 2004).

Besides several genetic and molecular biomarkers, cells undergoing differentiation or reprogramming processes are characterized by a metabolic plasticity based on activities involving endogenous fluorophores and likely affecting AF emission properties (Folmes *et al.*, 2012; Santin *et al.*, 2013) Figure 1. Mitochondria, in particular, play an essential role in the maintenance of stem cell homeostasis, consistently both with the switch from anaerobic to aerobic respiration during differentiation and with the autophagic processes, providing for the removal of undesired cell components to maintain the pluripotent status, the opposite occurring during the somatic to pluripotent cell reprogramming (Hernebring *et al.*, 2006; Wang *et al.*, 2011; Rehman *et al.*, 2010; Chen *et al.*, 2012). The consequent changes in the cell engagement in energetic metabolism influence the amount, redox state and bound-free condition of the coenzymes NAD(P)H and flavins (Croce *et al.*, 1999; Salmon *et al.*, 1982; Kunz *et al.*, 1986). The AF emission properties of these endogenous fluorophores up

to now mainly investigated in energetic metabolism studies (Aubin, 1979; Balaban and Mandel, 1990), have been more recently considered for the assessment of the stemness status of human and animal stem cells. Novel and sophisticated techniques have been applied, including a two photon non invasive autofluorescence imaging tool and a phasor approach for the monitoring of the metabolic state of different living stem cell models (Uchugonova *et al.*, 2008; Rice *et al.*, 2010; König *et al.*, 2011; Stringari *et al.*, 2011; Stringari *et al.*, 2012a,b; Santin *et al.*, 2013). The autophagic activity for the removal of undesired subcellular structures, in turn, is expected to result in an accumulation of lipofuscin like products, that can be detected though their AF emission in the yellow-reddish region (Wolman, 1980; Terman *et al.*, 2006).

The development of regenerative therapies is greatly relying on the use pluripotent cells (Welling and Geijsen, 2013). The induction of pluripotent stem cells (iPS) through the reprogramming of adult elements (Yamanaka, 2009; Cherry and Daley, 2012; Kahler *et al.*, 2013) is likely to be preferred to the use of Embryonic Stem Cells (ESCs), their self-renewal features being retained as long as the culture conditions prevent differentiation, along with the ability to differentiate into all adult cell types through their aggregation into embryoid bodies (EBs) (Evans *et al.*, 1981; Williams *et al.*, 1988; Desbaillets *et al.*, 2000). The use of iPS cells results in enormous advantages since it overcomes the ethical concerns related to the use of human ESCs and, at the same time, it allows in principle to generate pluripotent cells from a broad spectrum of adult somatic cells.

The successful driving of a cell lineage to the desired phenotype entails the correct assessment and monitoring of the stemness status. In this view, the AF analysis can provide data on the metabolic engagement, useful to integrate the transcription and surface-immunological biomarkers as the expression of regulation factors (Nagano *et al.*, 2008; Enver *et al.*, 2009), or at least to characterize cells from animal species for which immunomarkers are not yet available.

In our work we used pig iPS cells, currently highly considered for applications in biomedical and biotechnological fields, and EBs derived from them, to investigate the potential of real time, in vivo and non invasive AF analysis as a supportive tool for a comprehensive assessment and monitoring of the actual differentiation degree.

Materials and Methods

Cell model

Pig iPS cells have been maintained as previously described (Ezashi T *et al.*, PNAS 2009). In brief, pig iPS cells have been grown onto a feeder of inactivate mouse embryonic fibroblasts (MEF) in a medium based on DMEM/F12 and supplemented with 20% Knockout Serum Replacement, Glutamine, non-essential amino acids and basic FGF (4 ng/mL).

To obtain EBs, iPS cells have been first passaged onto gelatin-coated dishes (0.1%) to deplete the MEF feeder in pluripotency medium, and then passaged using Dispase (1 mg/mL) and plated onto ultra-lo attachment plated in a medium containing fetal bovine serum (FBS).

For both AF imaging and microspectrofluorometric analysis, the cells were seeded onto 0.1% gelatin coated glass coverslips in the absence of feeder, to be put upside down immediately before the AF imaging and microspectrofluorometric analyses.

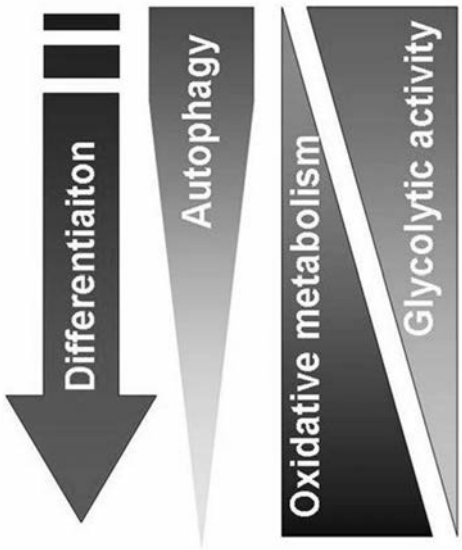

Figure 1. Schematic representation of metabolic signatures and their changes, exploitable for the AF analysis of cell differentiation: aerobic/anaerobic energetic metabolism and endocytosis/autophagy, involving respectively NAD(P)H and flavins, or lipofuscins as endogenous fluorophores.

Autofluorescence image analysis

The AF images were collected by means of an Olympus BX51 fluorescence microscope (Olympus Optical Co. GmBH, Hamburg, Germany), equipped with a 100W Hg excitation lamp and a 4.1 Mpixel digital photocamera (Olympus Camedia C-4040 zoom), the acquisition conditions being: WU Olympus fluorescence cube (330–385 nm band-pass excitation filter, Full Width at Half Intensity Maximum (FWHM) 58 nm), BA420 long-pass barrier filter; oil immersion 100X UplanFl Olympus objective (NA 1.25). Following each AF image collection, bright field pictures were also recorded from the same cells.

Microspectrofluorometric analysis

The AF spectra were recorded under epi-illumination by means of a microspectrograph (Leitz, Wetzlar, Germany) equipped with an Optical Multichannel Analyzer (EG&G - PAR, Princeton, NJ), and a 512-element intensified diode array detector, mod. 1420/512. Excitation light was provided by a 100 W Hg lamp (Osram, Berlin, Germany), combined with KG1-BG38 anti-thermal filters. Acquisition conditions were: 366 nm band-pass interference excitation filter (FWHM 10 nm, $T\%_{366} = 25$), 390 nm dichroic mirror ($T\%_{366} < 2$); 390 nm long pass filter; oil immersion 95X Leitz objective with incorporated iris diaphragm (NA 1.10-1.32).

Spectra were recorded in the 400-680 nm range, 10 sequential scans of 200 ms each for a total of 2 s of acquisition time. To avoid photobleaching effects before measurement, cells were selected and focused at microscope under low bright field illumination.

An iterative non-linear curve-fitting procedure (PeakFit; SPSS Science, Chicago, IL, USA) based on the Marquardt-Levenberg algorithm (1963) was used for the analysis of AF spectra. The procedure is based on a combination of half-Gaussian Modified Gaussian (GMG) spectral functions describing the emission profile of each single fluorophore to evaluate their relative contribution to the overall emission, by means of subsequent adjustments to match the best fit for the experimental spectrum profile, as already described in detail (Croce *et al.*,1999; Croce *et al.*, 2004). The spectral parameters of the single fluorophores considered were: free NAD(P)H (peak center wavelength, λ = 463 nm; FWHM = 115 nm), bound NAD(P)H (λ = 444 nm; FWHM = 105 nm), flavins (λ = 526 nm; FWHM = 81 nm), porphyrins (λ = 635 nm; FWHM = 20 nm), proteins (emission tail, λ<440 nm) and lipofuscin-like lipopigments ($\lambda \approx 587$ nm; FWHM $\approx$ 80 nm). In the two latter cases, modifications of the spectral functions were allowed, due to the variability of the lipofuscin-like lipopigments emission profile in dependence of their heterogeneous chemical composition *i.e.*, proteins, lipids, carotenoids- oxidation and crosslink degree (Wolman, 1980). The goodness of fitting verified in terms of r^2 coefficient determination, and residual analysis. The relative contribution (%) of each fluorophore estimated from the spectra normalized to 100 (area value, a.u.) was then referred to the real values of the whole emission area. A minimum of 25 cells was measured for each cell type for each sample (minimum, 2 slides).

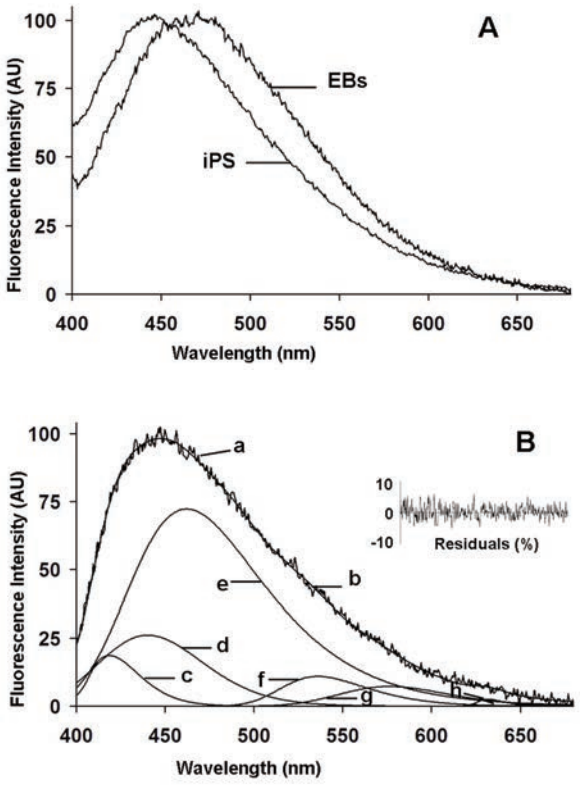

Figure 2. (A) Examples of AF spectra collected from iPS cells and EBs. (B) Example of fitting analysis of an AF spectrum collected from iPS cells. Measured spectrum (a) and calculated curve (b), as the sum of the contribution of the single endogenous fluorophores: proteins (c), NAD(P)H bound (d), NAD(P)H free (e), flavins (f), lipofuscin-like lipopigments (g), porphyrins (h). Insert: residual analysis. Fitting r^2 coefficient of determination ≥0.989.

Results

Microspectrofluorometric analysis

The AF spectra recorded from iPS and EB cells show differences in their emission profile (Figure 2A), that can be ascribed to changes in the relative contribution of the main endogenous fluorophores to the whole AF emission signal (Figure 2B). These changes have been analyzed by means of spectral fitting procedure and the results are presented as bar charts (Figure 3 A-C). In general, the greater contribution to the whole cell emission is given by the coenzyme NAD(P)H, accounting for more than 60%, oxidized flavins accounting for less than 4%, and lipofuscin-like lipopigments for a

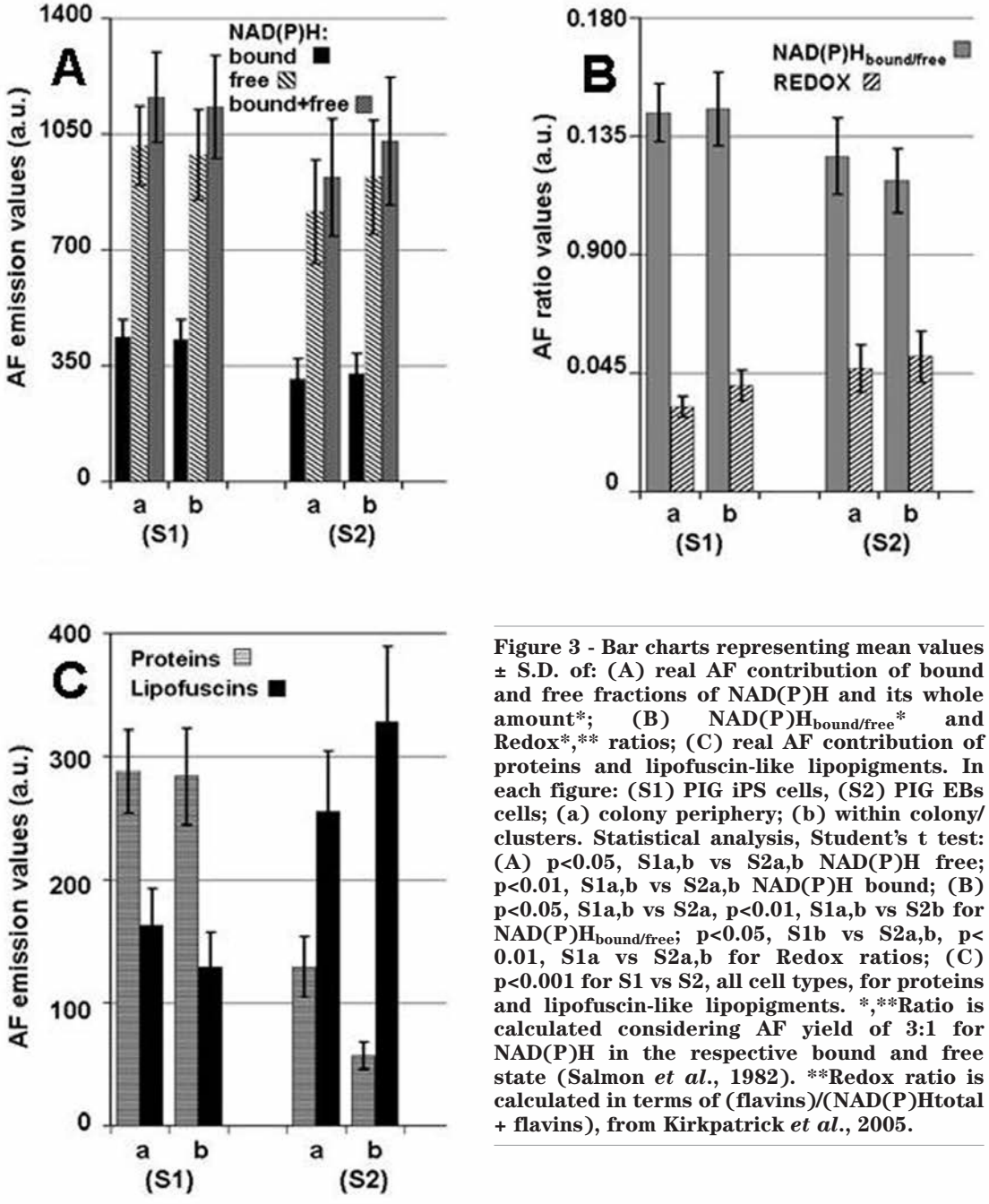

Figure 3 - Bar charts representing mean values ± S.D. of: (A) real AF contribution of bound and free fractions of NAD(P)H and its whole amount*; (B) $NAD(P)H_{bound/free}$* and Redox*, ratios; (C) real AF contribution of proteins and lipofuscin-like lipopigments. In each figure: (S1) PIG iPS cells, (S2) PIG EBs cells; (a) colony periphery; (b) within colony/clusters. Statistical analysis, Student's t test: (A) $p<0.05$, S1a,b vs S2a,b NAD(P)H free; $p<0.01$, S1a,b vs S2a,b NAD(P)H bound; (B) $p<0.05$, S1a,b vs S2a, $p<0.01$, S1a,b vs S2b for $NAD(P)H_{bound/free}$; $p<0.05$, S1b vs S2a,b, $p<0.01$, S1a vs S2a,b for Redox ratios; (C) $p<0.001$ for S1 vs S2, all cell types, for proteins and lipofuscin-like lipopigments. *,**Ratio is calculated considering AF yield of 3:1 for NAD(P)H in the respective bound and free state (Salmon *et al.*, 1982). **Redox ratio is calculated in terms of (flavins)/(NAD(P)Htotal + flavins), from Kirkpatrick *et al.*, 2005.**

fraction ranging from less than 10% to about 20%. The calculation of the real emission values of each single fluorophore indicates that, independently from the kind of cell considered within each sample, iPS cells in comparison to EBs cells show a greater content of NAD(P)H in parallel with higher NAD(P)$H_{bound/free}$ and lower redox ratio values (Figure 3 A-B). The contribution of lipofuscin-like lipopigments is less than a half in iPS cells with respect to EBs (Figure 3 C), and porphyrins are in general about 1%, except for a contribute for about 4% in the cells localizing at the periphery of EBs (*data not shown*).

Imaging of iPS and EB cells

Images recorded under the near UV excitation from living iPS cells and EBs show fluorescent cytoplasms around dark nuclei. The cytoplasmic AF patterns are characterized by a low and diffuse signal and distinct bluish bright particles, more numerous, evenly distributed and of comparable size in iPS cells than in EBs. Particles with a yellowish and brighter emission signal, a more variable size and uneven distribution can be also observed, more frequently in EBs than in iPS cells (Figure 4).

Discussion

Studies on the role of cell redox balance in the modulation of stemness status and differentiation have recently brought attention to the coenzymes NAD(P)H and flavins, that can act as intrinsic biomarkers because of their participation to energy production, reductive biosynthesis, and antioxidant defense (Uchugonova *et al.*, 2008; Ogasawara and Zhang, 2009; Hamanaka and Chandel, 2010;

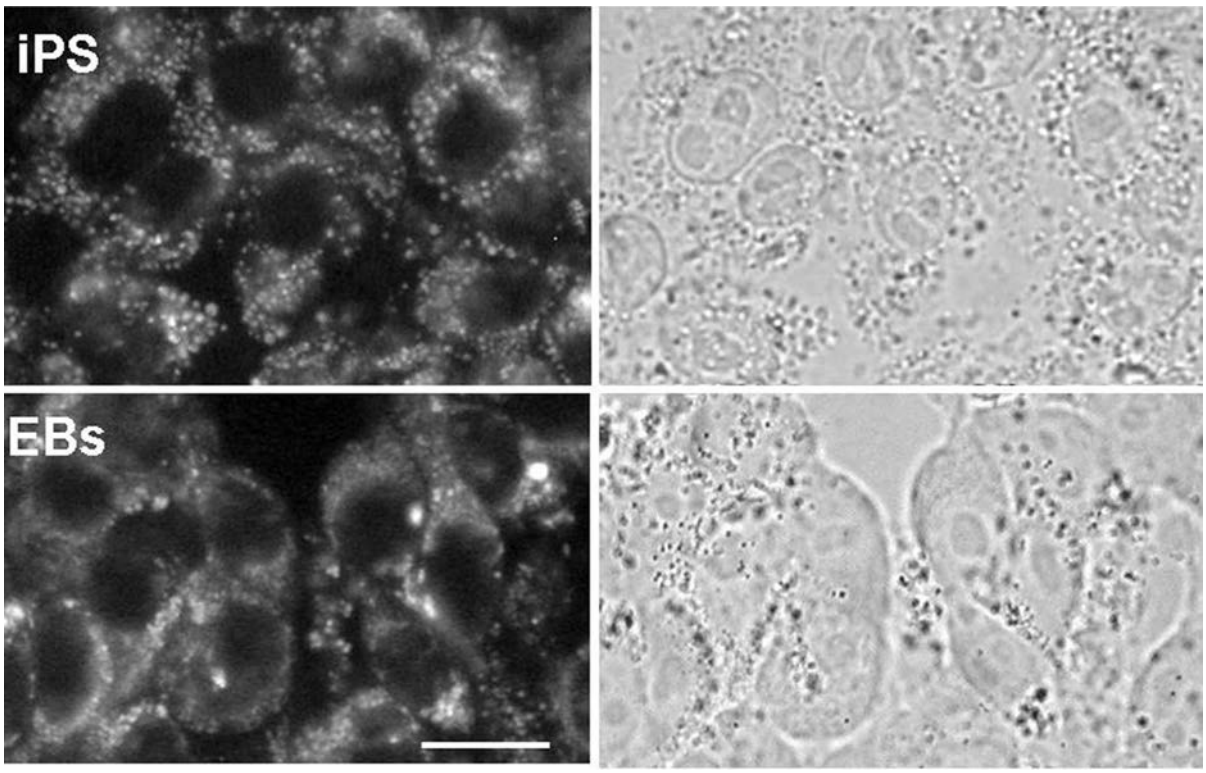

Figure 4. Examples of the AF distribution patterns and corresponding bright field images collected from living iPS cells and EBs. Each pair of images allows to appreciate a cytoplasmic diffuse AF emission signal around the dark nuclei. In comparison with EBs, iPS cells show more numerous bright bluish particles, evenly distributed and of comparable size, ascribable to mitochondria, while more brilliant yellowish granules with variable size and uneven distribution, ascribable to lipofuscin-like lipopigments, are shown by EBs. Bar: 25 µm.

Rice *et al.*, 2010; König *et al.*, 2011; Stringari *et al.*, 2011; Stringari *et al.*, 2012b). Therefore, the AF properties of these coenzymes in terms of signal amplitude, spectral shape and distribution patterns can be expected to reflect possible differences in the engagement of iPS cells and EBs in redox metabolic pathways. Actually, a higher turnover rate between the reduced and oxidized forms of NAD(P)H and flavins in iPS cells with respect to EBs is indicated by their greater content in NAD(P)H, accompanied by a higher NAD(P)H bound/free ratio and a lower redox ratio. These data suggest a still active engagement in aerobic metabolism of iPS cells, consistently with the results previously obtained in normal, young or immortalized fibroblasts (Croce *et al.*, 1999). The direct relationship between the relative increase in NAD(P)H in the bound with respect to the free state following the differentiation from progenitor to adult cell elements is further supported by comparable results on different cellular models undergoing differentiation both in culture and in their native environment (Stringari *et al.*, 2011; Stringari *et al.*, 2012a,b; Santin *et al.*, 2013).

The high redox ratio of EBs, in turn, is likely to be related to a still low turnover rate between reduced and oxidized forms of NAD(P)H and flavins during the switch from anaerobic to aerobic metabolism, with a rising in the engagement of mitochondria in state 3, the high level of oxidative metabolism producing ATP (Li *et al.*, 2009).

The differences in the energetic metabolism engagement suggested by the microspectrofluorometric analysis of our samples are supported by the AF images, able to show more numerous mitochondria in iPS cells than in EBs in the absence of exogenous dyes, because of intrinsic NADH emission. Lipofuscin-like lipopigments contribute to the cell AF emission in the yellow-red region. As a consequence, these fluorophores can be exploited as additional AF biomarkers providing comprehensive information on the presence of waste material accumulated at the intracellular level, as a product of autophagy and oxidative stress damage (Terman *et al.*, 2005; Stolzing *et al.*, 2006; Rice *et al.*, 2010; Rehman, 2010; Terman *et al.*, 2010; Stringari *et al.*, 2012c; Santin *et al.*, 2013). Our results show a much greater amount of lipofuscin-like lipopigments in EBs with respect to iPS cells, in full agreement with the role of autophagic activity providing for the removal of undesired subcellular structures to maintain the cell stemness status (Hernebring *et al.*, 2006; Rehman *et al.*, 2010; Wang *et al.*, 2011; Chen *et al.*, 2012).

Porphyrins, namely Protoporphyrin IX, despite their very small presence can be detected by means of spectral fitting analysis because of their narrow band peaking at 630 nm (Moesta, 2001), distinguishable from the low emission tail of the other fluorophores in the red region. In our samples the highest presence of porphyrins detected in cell clusters of EBs can be explained considering the porphyrin role as intermediates of the synthesis of heme-proteins, such as microsomial or mitochondrial cytochromes. Actually, a direct association between cytochrome *c* synthesis and cardiomyocyte differentiation has been demonstrated (Chen *et al.*, 2012), and an increase in the presence of porphyrins has been found during the transition from anaerobic to aerobic metabolism in mice stem cells (Santin *et al.*, 2013).

Conclusions

The AF results indicate that reprogrammed suine iPS cells do not show a complete recovery of the typical metabolic functions of the undifferentiated status. This finding could be related to the fact that suine iPS cells could not be equivalent to the naive mouse embryoid stem cells (Santin *et al.*, 2013). These results support the ability of AF analysis to assess stem cell differentiation degree and open a new perspective for the application of this technique as a supportive tool to investigate genetic and molecular biomarkers, both in already characterized models or in animal species of interest in veterinary, zootechnology, and more generally in developing research, even when immune-biomarkers are not available (Nowak-Imialek and Niemann, 2012)

Acknowledgments

We thank “Superpig Program” as a project co-financed by Lombardy Region through the “Fund for promoting institutional agreements” for supporting this work. We are also grateful to Prof. Michael Roberts (University of Missouri), for providing the pig iPS cell lines.

References

Aubin JE. Autofluorescence of viable cultured mammalian cells. J Histochem Cytochem 1979;27:36-43.

Balaban RS, Mandel LJ. Optical methods for the study of metabolism in intact cell. In: Forskett JK, Grinstein S, eds. Non-invasive Techniques in Cell Biology. New York USA: Wiley Liss, 1990:213-36.

Bottiroli G, Croce AC. Autofluorescence spectroscopy of cells and tissues as a tool for biomedical diagnosis. Photochem Photobiol Sci 2004;3:189-210.

Chen CT, Hsu SH, Wei YH. Mitochondrial bioenergetic function and metabolic plasticity in stem cell differentiation and cellular reprogramming. Biochim Biophys Acta 2012;1820:571-6.

Cherry AB, Daley GQ. Reprogramming cellular identity for regenerative medicine. Cell 2012;148:1110-22.

Croce AC, Ferrigno A, Vairetti M, Bertone R, Freitas I, Bottiroli G. Autofluorescence properties of isolated rat hepatocytes under different metabolic conditions. Photochem Photobiol Sci 2004;3:920-6.

Croce AC, Spano A, Locatelli D, Barni S, Sciola L, Bottiroli G. Dependence of fibroblast autofluorescence properties on normal and transformed conditions. Role of the metabolic activity. Photochem Photobiol 1999;69:364-74.

Desbaillets I, Ziegler U, Groscurth P, Gassmann M. Embryoid bodies: an in vitro model of mouse embryogenesis. Exp Physiol 2000;85:645-51.

Enver T, Pera M, Peterson C, Andrews PW. Stem cell states, fates, and the rules of attraction. Cell Stem Cell 2009;4:387-97.

Evans MJ, Kaufman MH. Establishment in culture of pluripotential-cells from mouse embryos. Nature 1981;292:154-6.

Ezashi T, Telugu BP, Alexenko AP, Sachdev S, Sinha S, Roberts RM. Derivation of induced pluripotent stem cells from pig somatic cells. Proc Natl Acad Sci U S A 2009;106:10993-8.

Folmes CDL, Dzeja PP, Nelson TJ, Terzic A. Energy metabolism plasticity enables stemness programs. Ann N Y Acad Sci 2012;1254:82-9.

Hamanaka RB, Chandel NS. Mitochondrial reactive oxygen species regulate cellular signaling and dictate biological outcomes. Trends Biochem Sci 2010;35: 505-3.

Hernebring M, Brole´n G, Aguilaniu H, Semb H, Nystro T. Elimination of damaged proteins during differentiation of embryonic stem cells. PNAS 2006;103: 7700-5.

Kahler DJ, Ahmad FS, Ritz A, Hua H, Moroziewicz DN, Sproul AA, et al. Improved methods for reprogramming human dermal fibroblasts using fluorescence activated cell sorting. PLoS One 2013;8:e59867.

Kirkpatrick ND, Zou C, Brewer MA, Brands WR, Drezek RA, Utzinger U. Endogenous fluorescence spectroscopy of cell suspensions for chemopreventive drug monitoring. Photochem Photobiol 2005;81:125-34.

König K, Uchugonova A, Gorjup E. Multiphoton fluorescence lifetime imaging of 3D-stem cell spheroids during differentiation. Microsc Res Tech 2011;74:9-17.

Kunz WS. Spectral properties of fluorescent flavoproteins of isolated rat liver mitochondria. FEBS 1986;195:92-6.

Li LZ, Zhou R, Xu HN, Moon L, Zhong T, Kim EJ, et al. Quantitative magnetic resonance and optical imaging biomarkers of melanoma metastatic potential. Proc Natl Acad Sci USA 2009; 106:6608-13.

Marquardt DW. An algorithm for least-squares estimation of non-linear parameters. J Soc Indust Appl Math 1963;11:431-41.

Moesta KT, Ebert B, Handke T, Nolte D, Nowak C, Haensch WE, et al. Protoporphyrin IX occurs naturally in colorectal cancers and their metastases. Cancer Res 2001;61:991-9.

Nagano K, Yoshida Y, Isobe T. Cell surface biomarkers of embryonic stem cells. Proteomics 2008;8:4025-35.

Nowak-Imialek M, Niemann H. Pluripotent cells in farm animals: state of the art and future perspectives. Reprod Fertil Dev 2012;25:103-28.

Ogasawara MA, Zhang H. Redox regulation and its emerging roles in stem cells and stem-like cancer cells. Antioxid Redox Signal 2009;11:1107-22.

Ramanujam N. Fluorescence spectroscopy in vivo. In: Meyers RA, ed. Encyclopedia of analytical chemistry. Chichester UK: John Wiley and Sons, 2000:20-56.

Rehman J. Empowering self-renewal and differentiation: the role of mitochondria in stem cells. J Mol Med 2010;88:981-6.

Rice WL, Kaplan DL, Georgakoudi I. Two-photon microscopy for non-invasive, quantitative monitoring of stem cell differentiation. PLoS One 2010;5:e10075.

Salmon JM, Kohen E, Viallet P, Hirscheberg JG, Wouters AW, Kohen C, et al. Microspectrofluorometric approach to the study of free/bound NAD(P)H ratio as metabolic indicator in various cell types. Photochem Photobiol 1982;36:585-93.

Santin G, Paulis M, Vezzoni P, Pacchiana G, Bottiroli G, Croce AC. Autofluorescence properties of murine embryonic stem cells during spontaneous differentiation phases. Lasers Surg Med 2013;45:597-607.

Stolzing A, Sethe S, Scutt AM. Stressed stem cells: temperature response in aged mesenchymal stem cells. Stem Cells Dev 2006;15:478-87.

Stringari C, Cinquin A, Cinquin O, Digman MA, Donovan PJ, Gratton E. Phasor approach to fluorescence lifetime microscopy distinguishes different metabolic states of germ cells in a live tissue. Proc Natl Acad

Sci U S A 2011;108:13582-7.
Stringari C, Edwards RA, Pate KT, Waterman ML, Donovan PJ, Gratton E. Metabolic trajectory of cellular differentiation in small intestine by Phasor Fluorescence Lifetime Microscopy of NADH. Sci Rep 2012a;2:568. doi: 10.1038/srep00568.
Stringari C, Nourse JL, Flanagan LA, Gratton E. Phasor fluorescence lifetime microscopy of free and protein-bound NADH reveals neural stem cell differentiation potential. PLoS One 2012b;7:e48014.
Stringari C, Sierra R, Donovan PJ, Gratton E. Label-free separation of human embryonic stem cells and their differentiating progenies by phasor fluorescence lifetime microscopy. J Biomed Opt. 2012c;17:046012-1-11, doi: 10.1117/1.JBO.17.4.046012.
Terman A, Brunk UT. Autophagy in cardiac myocyte homeostasis, aging, and pathology. Cardiovasc Res. 2005;68:355-65.
Terman A, Gustafsson B, Brunk UT. Mitochondrial damage and intralysosomal degradation in cellular aging. Mol Aspects Med 2006;27:471-82.
Terman A, Kurz T, Navratil M, Arriaga EA, Brunk UT. Mitochondrial turnover and aging of long-lived postmitotic cells: the mitochondrial–lysosomal axis theory of aging. Antioxid Redox Signal 2010;12:503-35.
Uchugonova A, König K. Two-photon autofluorescence and second-harmonic imaging of adult stem cells J Biomed Opt 2008;13:054068. doi:10.1117/1.3002370.
Wang J, Alexander P, McKnight SL. Metabolic specialization of mouse embryonic stem cells. Cold Spring Harb Symp Quant Biol 2011;76:183-93.
Welling M, Geijsen N. Uncovering the true identity of naïve pluripotent stem cells. Trends Cell Biol 2013;23:442-8.
Williams RL, Hilton DJ, Pease S, Willson TA, Stewart CL, Gearing DP, Wagner EF, Metcalf D, Nicola NA, Gough NM. Myeloid leukaemia inhibitory factor maintains the developmental potential of embryonic stem cells. Nature 1988;336:684-7.
Wolman M. Lipid pigments (chromolipids): their origin, nature and significance. Pathobiol Ann 1980;10:253-67.
Yamanaka S. A fresh look at iPS cells. Cell 2009;137:13-7.